THE JOURNAL OF BIOLOGICAL CHEMISTRY VOL. 289, NO. 4, pp. 2450–2456, January 24, 2014

Electric Stimulus Opens Intercellular Spaces in Skin*

Received for publication, August 28, 2013, and in revised form, December 3, 2013 Published, JBC Papers in Press, December 16, 2013, DOI 10.1074/jbc.M113.514414

Susumu Hama[‡1], Yuki Kimura[‡1], Aya Mikami[‡], Kanako Shiota[‡], Mao Toyoda[‡], Atsushi Tamura[§], Yukio Nagasaki[§], Kiyoshi Kanamura[¶], Kazuaki Kajimoto[‖], and Kentaro Kogure[‡2]

From the [‡]Department of Biophysical Chemistry, Kyoto Pharmaceutical University, Kyoto 607-8414, Japan, the [§]Graduate School of Pure and Applied Sciences, University of Tsukuba, Ibaraki 305-8573, Japan, [¶]TTI ellebeau Inc., Tokyo 140-0002, Japan, and the [‖]Faculty of Pharmaceutical Sciences, Hokkaido University, Sapporo 060-0812, Japan

Background: Although skin is a tight barrier, transdermal liposome delivery is achievable by faint electric stimulus (ES).
Results: ES caused rigid nanoparticle penetration into the epidermis, and induced connexin 43 phosphorylation, actin fiber depolymerization and Ca^{2+}-influx.
Conclusion: Our data indicate that ES opens epidermis intercellular spaces via intracellular signaling activation.
Significance: Skin barrier permeability could be controlled by ES via changes in cutaneous physiological properties.

Iontophoresis is a technology for transdermal delivery of ionic small medicines by faint electricity. Since iontophoresis can noninvasively deliver charged molecules into the skin, this technology could be a useful administration method that may enhance patient comfort. Previously, we succeeded in the transdermal penetration of positively charged liposomes (diameters: 200–400 nm) encapsulating insulin by iontophoresis (Kajimoto, K., Yamamoto, M., Watanabe, M., Kigasawa, K., Kanamura, K., Harashima, H., and Kogure, K. (2011) *Int. J. Pharm.* 403, 57–65). However, the mechanism by which these liposomes penetrated the skin was difficult to define based on general knowledge of principles such as electro-repulsion and electro-osmosis. In the present study, we confirmed that rigid nanoparticles could penetrate into the epidermis by iontophoresis. We further found that levels of the gap junction protein connexin 43 protein significantly decreased after faint electric stimulus (ES) treatment, although occludin, CLD-4, and ZO-1 levels were unchanged. Moreover, connexin 43 phosphorylation and filamentous actin depolymerization *in vivo* and *in vitro* were observed when permeation of charged liposomes through intercellular spaces was induced by ES. Ca^{2+} inflow into cells was promoted by ES with charged liposomes, while a protein kinase C inhibitor prevented ES-induced permeation of macromolecules. Consequently, we demonstrate that ES treatment with charged liposomes induced dissociation of intercellular junctions via cell signaling pathways. These findings suggest that ES could be used to regulate skin physiology.

Noninvasive transdermal delivery has many advantages for administering medication, such as avoiding a first pass effect, maintenance of stable blood concentrations, and reducing pain. Thus, transdermal delivery appears to be a superior administration method for clinical therapy. However, the transdermal penetration of exogenous materials including medicines is difficult, since skin represents a tight barrier. Various technologies have been developed to enhance transdermal drug penetration and delivery, including chemical enhancers such as menthol and ethanol, and physical acceleration methods such as electroporation.

Iontophoresis (IP)[3] is a noninvasive technology that physically enhances transdermal penetration of ionic medicines using faint electricity (1). Thus, faint electric stimulus (ES) is driving force for transdermal migration of ionic substances by IP. IP was generally considered to be effective only for charged amphiphilic small molecules such as methotrexate, dexamethasone, buspirone, and diclofenac (2–5). However, *in vivo* iontophoretic transdermal delivery of hydrophilic macromolecules including cationic liposomes, siRNA, and oligonucleotides, was recently successfully achieved (6–10). Despite these recent successes, the mechanism by which macromolecules penetrate through the skin is difficult to explain using general knowledge of principles such as electro-repulsion and electro-osmosis (1).

Beyond the stratum corneum, intercellular junctions such as tight junctions and adherens junctions are thought to present barriers to transdermal drug delivery. The functional proteins of these intercellular junctions are known to be sensitive to physical and chemical stimuli (11, 12). Furthermore, in cardiac muscle cells the gap junction-associated protein connexin 43 (Cx43) responded to electric stimulus, which was followed by changes in intercellular adhesion (13). In addition, cationic macromolecules such as poly-arginine and poly-lysine were reported to induce dysfunction of tight junctions and enhance paracellular permeability (14).

In the present study, we hypothesized that faint electric stimulus (ES) with cationic liposomes would induce intercellular

* This work was supported by a Grant-in-Aid for Scientific Research on Innovative Areas, Nanomedicine Molecular Science (No. 2306) from Ministry of Education, Culture, Sports, Science, and Technology of Japan.
[1] These authors contributed equally to this study.
[2] To whom correspondence should be addressed: Department of Biophysical Chemistry, Kyoto Pharmaceutical University, Kyoto, 607-8414, Japan. Tel.: 81-75-595-4663; Fax: 81-75-595-4762; E-mail: kogure@mb.kyoto-phu.ac.jp.

[3] The abbreviations used are: IP, iontophoresis; ES, imperceptible electric stimulus; Cx43, connexin 43; SD, Sprague Dawley; NHEK, Normal human epidermal keratinocyte; DOTAP, 1,2-dioleoyl-3-trimethylammonium-propane; Rh-PE, 1,2-dioleoyl-sn-glycero-3-phosphoethanolamine-*N*-(lissamine rhodamine B sulfonyl); EPC, egg phosphatidylcholine; Chol, cholesterol; TER, transepithelial electrical resistance; LY, lucifer yellow; CLD-4, claudin-4; PKC, protein kinase C; DOPE, 1,2-dioleoylphosphatidylethanolamine.

space apertures by altering intercellular junctions. We examined the effect of ES on intercellular junctions such as tight junctions and gap junctions *in vitro* and *in vivo*. We also evaluated the effect of ES on intracellular events, including protein phosphorylation and changes in intracellular signaling factors. Findings from this study will be useful for understanding dermal physiology from a novel perspective and developing efficient noninvasive transdermal drug delivery systems.

EXPERIMENTAL PROCEDURES

Animals and Cells—Sprague-Dawley (S.D.) rats (male, 6 weeks old) were purchased from Japan SLC, Inc. (Shizuoka, Japan). Normal human epidermal keratinocyte (NHEK) cells and Caco-2 cells were obtained from Kurabo Industries Ltd. (Osaka, Japan) and the RIKEN Bioresource Center (Wako, Japan), respectively. All animals were maintained and used in accordance with the animal protocol approved by the Institutional Animal Care and Use Committee, Kyoto Pharmaceutical University (Kyoto, Japan).

Materials—1,2-Dioleoyl-3-trimethylammonium-propane (DOTAP) and 1,2-dioleoyl-sn -glycero-3-phosphoethanolamine-*N*-(lissaminerhodamine B sulfonyl) (Rh-PE) were purchased from Avanti Polar Lipids (Alabaster, AL). Egg phosphatidylcholine (EPC) was obtained from the NOF Corporation (Tokyo, Japan). Cholesterol (Chol) was purchased from Nacalai Tesque (Kyoto, Japan). The devices for *in vivo* iontophoresis (TCTTM) were manufactured by TTI ellebeau Inc. (Tokyo, Japan). Red Dot^{TM} electrodes for *in vitro* electric stimulus were purchased from 3M Health Care, Ltd. (Loughborough, UK). The rabbit anti-occludin polyclonal antibody was purchased from ZYMED laboratory (San Francisco, CA). The mouse anti-claudin-4 monoclonal antibody and the Alexa 488 and Alexa 594 labeled secondary antibodies for immunohistochemistry were from Invitrogen (Carlsbad, CA). The rabbit anti-ZO-1 polyclonal antibody and the mouse anti-Cx43 monoclonal antibody were from Santa Cruz Biotechnology, Inc. (Santa Cruz, CA). The rabbit anti-Cx43 (Phospho-Ser367) polyclonal antibody was from Signalway Antibody Co., Ltd. (Pearland, TX). Rhodamine-phalloidin for F-actin staining was from Cytoskeleton, Inc. (Denver, CO).

Liposome Preparation—DOTAP-based cationic liposomes were prepared as described previously (8). Briefly, DOTAP/EPC/Chol (4:4:2 molar ratio) were mixed in chloroform and dried to a thin lipid film using nitrogen gas. The lipid film was hydrated with 10 mM HEPES buffer (pH 7.4) followed by sonication in a bath-type sonicator (AU-25C, Aiwa, Tokyo, Japan). The final lipid concentration of the prepared liposomes was 25 mM. Measurement of liposome physicochemical properties with a Zetasizer Nano (Malvern Instruments Ltd., UK) showed that the liposome particle diameter and ζ-potential were 100–200 nm and +50 to +70 mV, respectively. Fluorescent dye-labeled liposomes were also prepared as described above, except that Rh-PE was added at a volume of 1 mol% of the final lipid concentration.

Iontophoresis (IP)—In vivo IP of liposomes was conducted according to our previous reports (8). Briefly, rats were anesthetized with pentobarbital sodium by intraperitoneal injection. For liposome administration, nonwoven fabric (0.785 cm^2) containing a suspension of cationic liposomes (5 mol lipids) or nanogels (60 mg/ml) was placed on the shaved dorsal skin and a second nonwoven fabric moistened with saline was placed 1 cm away. The nonwoven fabrics containing the nanoparticles and saline were connected to the anode and cathode, respectively, of a power supply (TTI ellebeau, Inc., model TCCR-3005, Tokyo, Japan) with Ag-AgCl electrodes and the connections were covered with tape. A current density of 0.48 mA/cm^2 was applied for a 1 h. Then, the skin was excised at immediately (0 h), 3 h or 6 h after current application (IP), and used for preparation of cross section or samples of Western blotting. *In vitro* electric stimulus of liposomes was also carried out as described above, except that Red Dot^{TM} electrodes were used.

Confocal Laser Scanning Microscopy (CLSM)—To evaluate immunostaining and liposome delivery, skin tissue from rats after IP was embedded into O.C.T compound and tissue sections (16 μm thickness) were prepared with a LEICA CM1100 cryostat (Leica Microsystems, Germany). Images were obtained by confocal laser scanning microscopy with a LSM 510 META microscope (Carl Zeiss Co. Ltd.) equipped with an objective lens (EC Plan-Neofluar 10X/0.3 M27) or an oil-immersion objective lens (Plan-Apochromat 63/NA1.4).

Cell Culture—NHEK cells were cultured in HuMedia-KG2 medium (Kurabo Industries Ltd., Osaka, Japan) containing 10 μg/ml insulin, 0.1 ng/ml human epidermal growth factor, 0.5 μg/ml hydrocortisone, 50 μg/ml gentamicin, 50 ng/ml amphotericin, and 0.4% *v*/*v* bovine pituitary extract. These cells were used for immunohistochemical analysis. Caco-2 cells were maintained in Dulbecco's modified Eagle's medium (DMEM) containing non-essential amino acids, 10% fetal bovine serum (FBS), 1% penicillin, and streptomycin. This cell line was used for immunohistochemical analysis as well as barrier function and permeability assays.

Western Blotting—Isolated skin tissues were subjected to frost shattering and then treated with lysis buffer (25 mM Tris-HCl (pH 6.5), 1% (v/v) glycerol, 1% (v/v) SDS, and 5% 2-mercaptoethanol). Protein content in the extracted samples was measured with BCA Protein Assay Reagent (Thermo Fisher Scientific Inc., Waltham, MA) and the samples loaded on 7–12% SDS-polyacrylamide gels. Proteins were separated by SDS-PAGE and electrophoretically transferred to PVDF membranes, which were then blocked with 5% nonfat dry milk in Tween solution (500 mM P_i buffer, 151 mM NaCl, 0.16% (v/v) Tween-20). The membrane was incubated with primary antibody (diluted according to the manufacturer's instructions) at room temperature and the corresponding HRP-conjugated secondary antibody diluted 1:2,000. The blots were detected using the ECL Western blotting Detection Reagent (GE Healthcare, Waukesha, WI) with a Versa Doc Imager 5000 (Bio-Rad Laboratories, Hercules, CA). Densitometric analysis was conducted with Quantity One software (ver. 4.5) (Bio-Rad). In this analysis α-tubulin protein was used as an internal control.

Immunohistochemistry—Following treatment, tissue sections or cells were fixed in phosphate-buffered saline (PBS) containing 4% paraformaldehyde for 15 min at room temperature, washed with PBS, permeabilized in PBS containing 1% Triton X-100 for 10 min at room temperature, and blocked in

PBS containing 0.5% FBS. Tissue sections or cells were then incubated with primary antibodies overnight at room temperature in a moist chamber. Alexa 488 conjugated anti-rabbit antibody or Alexa 594 conjugated anti-mouse antibody were used as secondary antibodies with 1 h incubation at 37 °C. After washing, tissue sections and cells were mounted in PBS containing 80% glycerol and VECTASHIELD with DAPI (Vector Laboratories, Inc., Burlingame, CA). The images were observed by CLSM as described above. To quantify the amount of proteins in the obtained images, the total immunoreactive pixel areas were analyzed with Lumina Vision software (ver. 3.1) (MAITANI, Co., Fukui, Japan).

Barrier Function and Permeability Assay—For transepithelial electrical resistance (TER), lucifer yellow (LY), and fluorescent-labeled liposome permeability assays, Caco-2 cells were seeded onto 12 mm transwells (3.0 μm pore size, Corning Inc., Corning, NY) and grown until the cellular monolayer reached confluence. The apical and basolateral chambers across the Caco-2 cell monolayers were pre-incubated in fresh medium at 37 °C for 1–2 h. TERs were measured by Millicell (Millipore, Billerica, MA). Permeability assays were conducted using the Caco-2 cell monolayers with the TER above 500 Ω/cm^2. The amount of LY and liposomes that penetrated from the apical chamber across the cell monolayer, and then into the basolateral chamber was determined as the fluorescence intensity by PLATE manager Infinite M200 (Tecan Systems Inc., San Jose, CA).

Evaluation of Intracellular Ca^{2+} Concentration—NHEK or Caco-2 cells were plated onto a 35-mm glass based dish (Asahi Glass Co. Ltd., Tokyo, Japan). After incubation for 24 h, the amount of intracellular Ca^{2+} was determined using a Fluo 4 calcium assay kit (Dojindo Laboratories, Tokyo, Japan) according to the manufacturer's instructions. Briefly, cells were treated with loading buffer containing Fluo 4-AM at 37 °C for 1 h. Following replacement of the buffer by recording medium, *in vitro* IP was conducted for 2 min as described above. The fluorescent signals corresponding to the amount of intracellular Ca^{2+} were observed with a fluorescence microscope (Olympus, Tokyo, Japan).

RESULTS

Nanoparticles Penetrate into the Skin by Iontophoresis—Although nano-sized particles would appear to be too large to be noninvasively penetrable into the skin by ES, cationic liposomes (diameter: ~200–400 nm, zeta-potential: ~50–70 mV) were observed in the skin after 3 h of iontophoresis (IP), and the liposome structure was maintained even after transfollicular delivery by IP (8). Here, the liposomes (red) were localized in hair follicles immediately after IP and penetrated into the skin 3 h after IP (Fig. 1*A*). Moreover, penetration into the skin of rigid cationic nanogel particles (15) having average diameters ranging from 55 to 425 nm was achieved within three hours of IP treatment. The smallest nanogel particles (55 nm) penetrated and localized in the epidermal layer (Fig. 1*B*), while larger particles (120–425 nm) were observed on the skin surface and not in the epidermis (data not shown). Based on this result, we hypothesized that the nanoparticles would permeate through intercellular spaces in the epidermal layer that are produced by

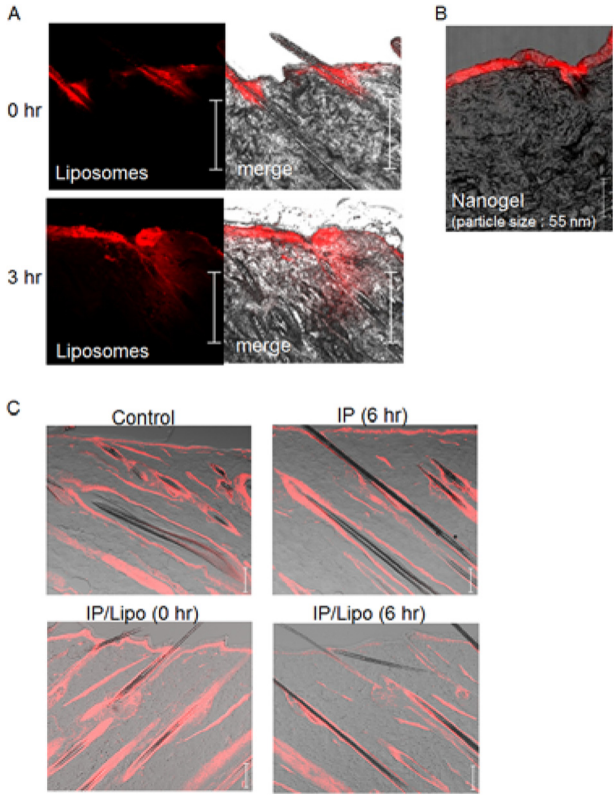

FIGURE 1. **Effects of IP with cationic liposomes on physiological conditions of rat dorsal skin.** *A*, time-dependent change in the distribution of rhodamine-labeled cationic liposomes (*red*) in the skin after IP treatment. *B*, IP-induced epidermal penetration of cationic nanogel labeled with rhodamine (*red*). *C*, phalloidin immunohistochemical analysis of F-actin (*red*) in the skin. Control means the intact skin without IP/liposome treatment. IP (6 h) means the skin at 6 h after IP without liposomes. IP/Lipo (0 h) and IP/Lipo (6 h) are the skins at 0 and 6 h after IP with liposomes. Bar indicates 100 μm.

ES-induced morphological and physiological changes in skin cells. Indeed, skin showed that levels of F-actin present as polymerized actin were decreased by IP treatment with liposomes (Fig. 1*C*), although significant change of F-actin in the skin was not recognized even at 6 h after IP treatment without liposomes (Fig. 1*C*). These results suggest that IP with liposomes induces dynamic changes that involve actin rearrangement in skin tissue.

Effects of IP on Intercellular Junction Proteins in Rat Skin—In the epidermal layer of skin tissue, intercellular spaces are closed by junction proteins. To obtain information regarding IP-induced changes in intercellular junctions in the skin, the amounts of proteins associated with tight and gap junctions were quantified by Western blot analysis. Significant changes in the amount of tight junction proteins, such as occludin, claudin-4 (CLD-4), and ZO-1 were not observed after IP treatment with/without liposomes (Fig. 2, *A*–*C*). In contrast, the amount of gap junction protein Cx43 (16) in the skin treated by IP with cationic liposomes was significantly lower than those of control topical application and control IP-treated skins, although no significant difference between control IP and IP/liposome treatments was observed (Fig. 2*D*). Since the degradation of Cx43 protein is known to be induced by Cx43 phosphorylation (17), we checked the phosphorylation status of Cx43 in IP-treated rat skin. As shown in Fig. 3*A*, p-Cx43/Cx43 was

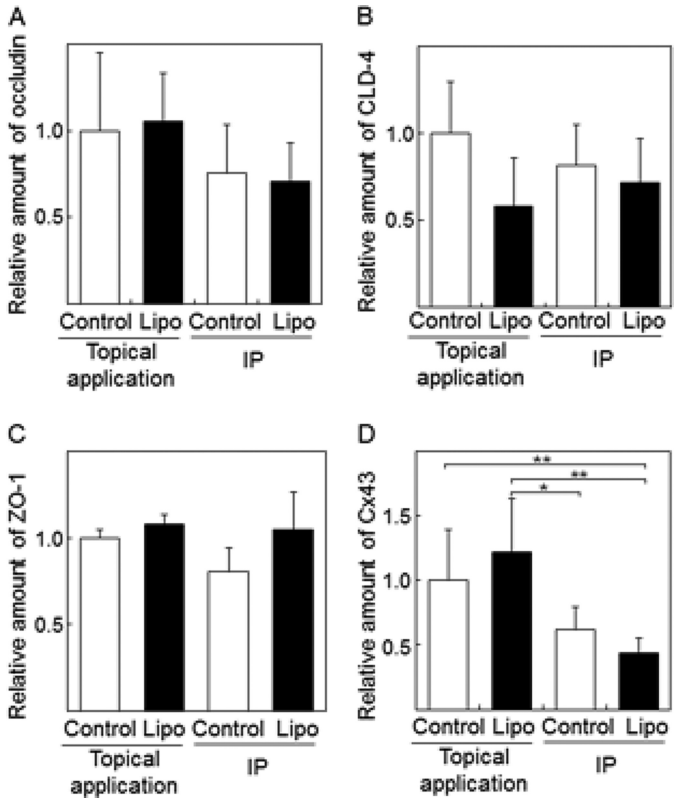

FIGURE 2. **Effects of IP with cationic liposomes on intercellular junction proteins in rat skin.** Western blot analysis and quantification of the tight junction proteins occludin (*A*), CLD-4 (*B*), ZO-1 (*C*), and gap junction protein Cx43 (*D*) in skin treated with IP with liposomes. The Control/topical application indicates treatment of skin surface with buffer. Control/IP means IP treatment with buffer. The data are represented as the average with standard deviation ($n > 3$). **, $p < 0.01$, *, $p < 0.05$.

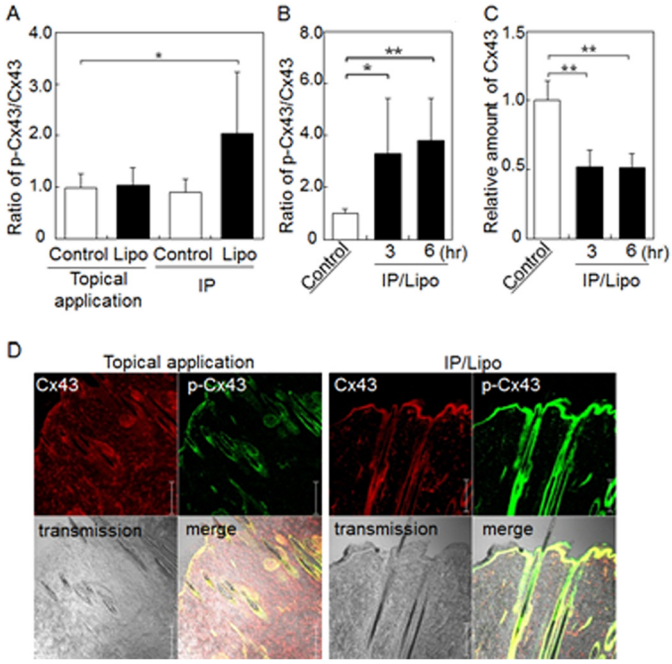

FIGURE 3. **IP with cationic liposomes induces Cx43 phosphorylation in rat skin.** Western blot analysis of the relative amount of phosphorylated Cx43 compared with total Cx43 in skin treated with liposomes followed by additional incubation for 0 h (*A*), and 3 or 6 h (*B*). *C*, Western blot analysis of the relative amount of total Cx43 in skin treated with liposomes followed by additional incubation for 3 or 6 h. *D*, immunohistochemical analysis of Cx43 (*red*) and phosphorylated Cx43 (*green*) in skin treated with IP with liposomes. The data are represented as the average with standard deviation ($n > 3$). **, $p < 0.01$, *, $p < 0.05$. Bar indicates 100 μm.

increased by IP with liposomes, although no significant difference between Cx43 relative amounts of control IP and IP/liposome was observed (Fig. 2*D*). It was suggested that the phosphorylation of Cx43 in the skin treated by IP/liposome was higher than that in the control IP-treated skin. Moreover, the increase in phosphorylated Cx43 and decrease in Cx43 levels were observed even 6 h after IP/liposome treatment (Fig. 3, *B* and *C*). Additionally, the IP/liposome-dependent increase in phosphorylated Cx43 and decrease in Cx43 levels were confirmed by immunohistochemical analysis of skin cross sections (Fig. 3*D*). Together, these results suggest that Cx43 phosphorylation induced by IP/liposomes triggers a decrease in Cx43 levels followed by opening of intercellular spaces in the epidermal layer of skin. On the other hand, there was no significant difference in Cx43 level in 3 and 6 h in Fig. 3*C*. It was assumed that regeneration of Cx43 protein might be occurred after decrease in the amount of Cx43 protein by enhancement of phosphorylation for recovering gap junction at 6 h after IP/liposome treatment.

Effect of ES on Intercellular Junctions of Cultured Cells in Vitro—To confirm whether the phenomena observed in the skin can be induced by ES in an *in vitro* culture cell system, the effect of ES with cationic liposomes on junction proteins in primary cultures of normal human epidermal keratinocytes (NHEK) was examined. Similar to the *in vivo* experiment, phosphorylated Cx43 appeared in NHEK cells after ES with liposomes, although levels of the tight junction protein ZO-1 were not changed by ES/liposome treatment (Fig. 4*A*). F-actin levels also decreased after ES treatment with liposomes, suggesting that F-actin depolymerization was induced by ES/liposomes (Fig. 4*A*).

To confirm the participation of Cx43 phosphorylation in forming apertures in intercellular spaces, the translocation of Lucifer yellow (LY), a model compound, or liposomes through cell monolayers was examined. Since primary cultured NHEK cells were not suitable for analyzing permeation of cell monolayers cultured on Transwell membranes, the human epithelium cell line Caco-2 was used. As shown in Fig. 4*B*, ZO-1 and CLD-4 were clearly observed at the boundary region of the Caco-2 cells. The tight junction proteins were not changed and, similar to NHEK cells, the amount of phosphorylated Cx43 also increased after ES with liposomes (Figs. 4*B* and 5*A*). The tightness of the cell monolayers on the Transwell membrane was sufficient, since transendothelial electrical resistance (TER) was very high (above 500 Ω/cm^2), although TER was reduced by ES treatment with/without liposomes (Fig. 5*B*). However, significant permeation of LY (MW: 480) and liposomes through cell layers was induced only by ES/liposome treatment (Fig. 5, *C* and *D*). Together, these results suggest that ES with ionic liposomes opens nanoparticle-permeable intercellular spaces.

Protein Kinase C Activation Triggers Apertures in the Intercellular Spaces Induced by ES—To clarify the mechanism by which apertures in the intercellular space are created by ES with ionic liposomes, we examined the effect of a protein kinase C (PKC) inhibitor on Cx43 phosphorylation, liposome transder-

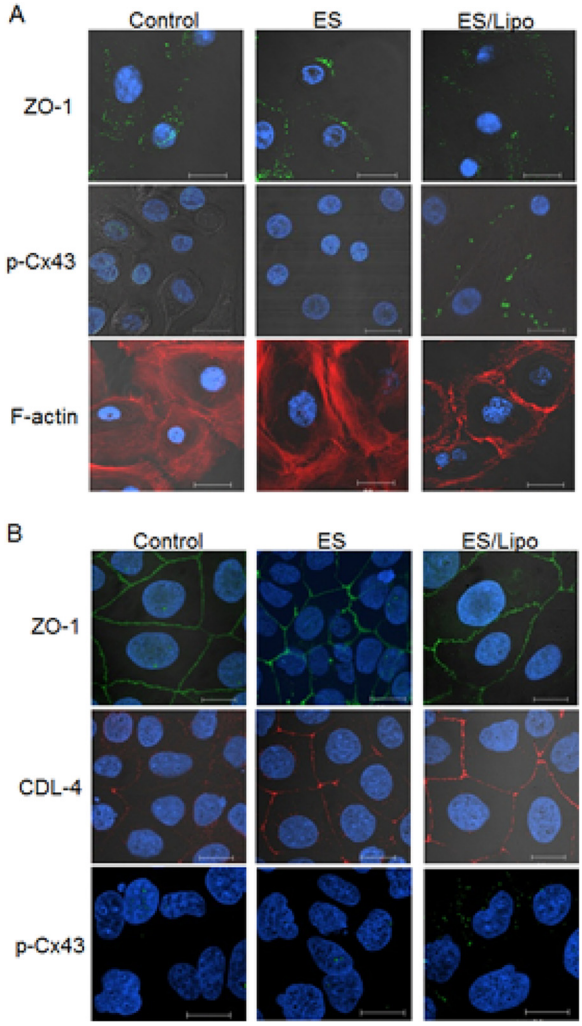

FIGURE 4. **Effect of ES with liposomes on intercellular junctions of cultured cells *in vitro*.** Immunohistochemical analysis of tight junction proteins ZO-1 (*green*) and CLD-4 (*red*) phosphorylated Cx43 (*green*) and F-actin (*red*) in (*A*) NHEK cells or (*B*) Caco-2 cells after ES treatment with/without liposomes. Bar indicates 20 μm. Nuclei were stained with 4′,6-diamidino-2-phenylindole (DAPI, *blue*).

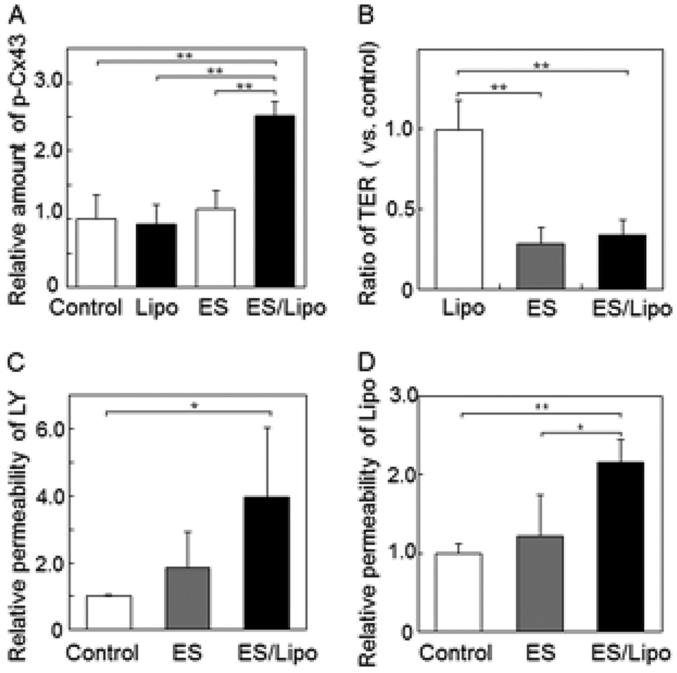

FIGURE 5. **ES/liposomes increase intercellular spaces in Caco-2 cell monolayers.** *A*, relative amount of phosphorylated Cx43 compared with total Cx43 in Caco-2 cells evaluated by Western blotting. Changes in TER (*B*) and permeability of LY (*C*) and liposomes (*D*) through Caco-2 cell monolayers on Transwell membranes treated with ES with cationic liposomes. The data represent the average with standard deviation ($n > 3$). **, $p < 0.01$, *, $p < 0.05$.

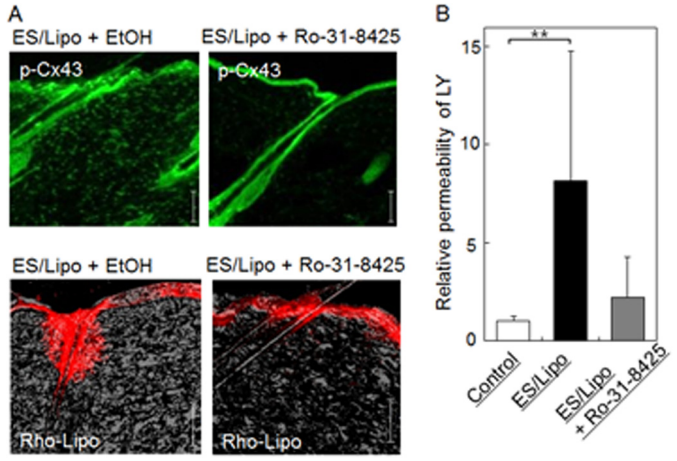

FIGURE 6. **Effects of a PKC inhibitor on the transdermal penetration of liposomes *in vivo* and relative permeability of LY *in vitro*.** Effect of a PKC inhibitor (Ro-31–8425) on (*A*) Cx43 phosphorylation (*green*) and transdermal penetration of liposomes (*red*) in skin treated with IP with liposomes and (*B*) permeation of LY through cultured cell monolayers treated with ES with liposomes. Bar indicates 100 μm. The data represent the average with standard deviation ($n > 3$).

mal penetration, and *in vitro* cell monolayer permeation, since PKC reportedly regulates Cx43 phosphorylation (18, 19). Pre-administration of the PKC inhibitor Ro-31–8425 into the skin by needle-free injection (20) reduced the amount of phosphorylated Cx43 and prevented transdermal liposome penetration (Fig. 6*A*). Similarly, the PKC inhibitor showed a tendency to inhibit enhanced LY permeation through cell monolayers (Fig. 6*B*). Moreover, since Ca^{2+} inflow into cells activates PKCs (21), the effect of ES/liposome treatment on the intracellular concentration of Ca^{2+} in Caco-2 and NHEK cells was examined. Fluorescent signals indicating the cellular Ca^{2+} concentration increased significantly after ES treatment with liposomes, especially in NHEK cells (Fig. 7). This increase in fluorescence could be prevented by the addition of EGTA, a Ca^{2+} chelator (Fig. 7). These results indicate that ES with liposomes induces Ca^{2+} influx into the cytoplasm.

DISCUSSION

In the present study, we analyzed the mechanism for noninvasive nanoparticle penetration through the skin by IP. Here liposomes acted as representative nanoparticles and were delivered in a time-dependent manner by IP to areas around the hair follicle and deeper regions of the skin. Liposome penetration into the skin was thought to be mediated by either a transcellular or paracellular route. Although fusogenic liposomes are known to be effective for drug delivery, liposomes consisting of DOTAP and 1,2-dioleoylphosphatidyl ethanolamine (DOPE) as the fusogenic lipid in IP-mediated administration have shown inferior penetration compared with that of DOTAP/EPC/Chol used in this study (8). We previously reported that

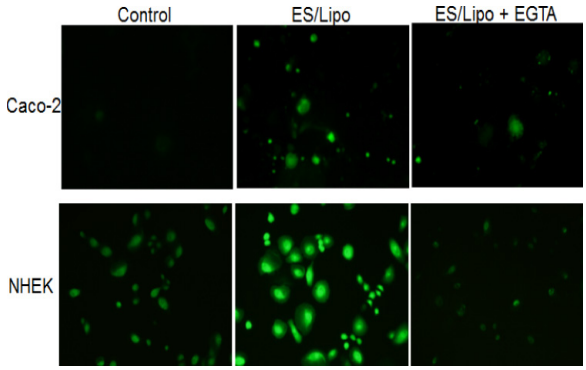

FIGURE 7. **ES/liposomes increase Ca^{2+} influx in cultured cells.** Ca^{2+} influx visualized by Fluo-4 AM (*green*) in NHEK and Caco-2 cells 2 min after ES/liposome treatment with/without pretreatment of chelator (EGTA).

liposomes penetrated as intact vesicles with IP (8) while in this study we showed that nanogels, non-fusogenic and rigid nanoparticles were also delivered into skin (Fig. 1*B*). Hence, the penetration of nanoparticles by IP is likely mediated by a paracellular route that does not involve a membrane fusion process. Regarding the penetration mechanism of liposomes via a paracellular route, El Maghraby *et al.* proposed that penetration of some liposomes having high flexibility, *i.e.* ultradeformable liposomes, are known to be involved in the hydration gradient and can undergo deformability-driven movement through small pores (22). However, the mechanism of nanoparticle penetration with ES likely differs from that without ES. Although the liposomes used in this study consisted of DOTAP/EPC/Chol, and show low plasticity due to the membrane stabilizing effect of cholesterol, these liposomes have an effective IP-mediated administration delivery capability than more flexible liposomes consisting of DOTAP/DOPE. In addition, since liposomes cannot penetrate into the skin by mere topical application, a paracellular-dependent mechanism for IP-induced penetration of liposomes would be difficult to explain by morphological changes in the liposomes. Cationic polymers such as protamine and chitosan were recently reported to enhance paracellular permeation by altering cytoskeleton and intercellular junctions (23, 24). In addition, depolymerization of F-actin induced enhancement of paracellular permeation following disassembly of intercellular junction proteins (25). In this study, depolymerization of F-actin was observed for IP with cationic liposomes (Figs. 1*C* and 4*A*) suggesting that the dermal structure and barrier function would be changed dramatically by interactions between cationic liposomes and skin component cells under ES.

For IP/liposome treatments, the amount of Cx43 decreased with Cx43 phosphorylation, although no significant changes in occludin, CLD-4 and ZO-1 levels were observed *in vivo* and *in vitro* (Figs. 2–4). These results suggest that the decrease in Cx43 participates in the enhanced permeation seen after IP/liposome treatment. Cx43 turnover is controlled by its phosphorylation status wherein phosphorylated Cx43 internalizes via clathrin-mediated endocytosis, and then is degraded in the endosome/lysosome (17). Thus, the decrease in Cx43 protein levels at the cell membranes may induce cleavage of gap junctions. In a previous report, the gap junction blocker 18β-glycyrrhetinic acid reduced barrier function and enhanced permeability of molecules through endothelial cells, suggesting that the aperture of intercellular spaces due to gap junction cleavage contributes to transdermal permeation of nanoparticles (26).

Activation of PKCα and Ca^{2+} influx was involved in the induction of transdermal permeation of liposomes *in vitro* and *in vivo* (Figs. 6 and 7). Since Ca^{2+} influx is required for PKCα activation, Ca^{2+} influx induced by ES/liposome treatment would likely activate PKCα. Thus, Ca^{2+} influx would be a key step for induction of transdermal permeation by ES. In the present study, cationic charge was necessary for transdermal permeation of liposomes, Cx43 phosphorylation and PKCα activation *in vitro* and *in vivo*. Since cationic liposomes may neutralize the cell membrane surface charge due to electrostatic interactions with negatively charged surface molecules such as heparan sulfate proteoglycan (27), the electrical balance between the inner and outer faces of the cell membrane tends toward inside negative. As such, anodal IP would induce the flow of cationic ions from the outside to the inside of cells. To cancel the imbalance in the membrane potential, Ca^{2+} forced by anodal IP might flow easily into the inside of the cells. This increase in intracellular Ca^{2+} concentration induced by IP with liposomes might activate PKC (21), which in turn induces Cx43 phosphorylation, resulting in gap junction dissociation (16, 26, 28). Moreover, since increases in cytoplasmic Ca^{2+} concentration are also suggested to induce F-actin depolymerization (29), cell-cell interactions via tight junctions and adherens junctions that connect with the cytoskeleton (30, 31) might be altered depending on changes in the F-actin polymerization state induced by ES/liposome treatment. Therefore, the aperture of intercellular spaces due not only to gap junction-cleavage, but also changes in tight and adherens junctions due to F-actin depolymerization may facilitate transdermal nanoparticle permeation.

In conclusion, we demonstrated that ES treatment with cationic liposomes induced dissociation of intercellular junctions, including gap junctions, tight junctions, and adherens junctions, via activation of cell signaling pathways that involve PKC activity mediated by Ca^{2+} influx. The findings in the present study suggest that the skin barrier could be controlled by ES with charged liposomes via changes in cutaneous physiological properties.

REFERENCES

1. Kalia, Y. N., Naik, A., Garrison, J., and Guy, R. H. (2004) Iontophoretic drug delivery. *Adv. Drug Deliv. Rev.* **56,** 619–658
2. Meidan, V. M., Al-Khalili, M., and Michniak, B. B. (2003) Enhanced iontophoretic delivery of buspirone hydrochloride across human skin using chemical enhancers. *Int. J. Pharm.* **264,** 73–83
3. Vemulapalli, V., Banga, A. K., and Friden, P. M. (2008) Optimization of iontophoretic parameters for the transdermal delivery of methotrexate. *Drug Deliv.* **15,** 437–442
4. Kigasawa, K., Kajimoto, K., Watanabe, M., Kanamura, K., Saito, A., and Kogure, K. (2009) In vivo transdermal delivery of diclofenac by ion-exchange iontophoresis with geraniol. *Biol. Pharm. Bull.* **32,** 684–687
5. Cázares-Delgadillo, J., Balaguer-Fernández, C., Calatayud-Pascual, A., Ganem-Rondero, A., Quintanar-Guerrero, D., López-Castellano, A. C., Merino, V., and Kalia, Y. N. (2010) Transdermal iontophoresis of dexamethasone sodium phosphate in vitro and in vivo: effect of experimental parameters and skin type on drug stability and transport kinetics. *Eur. J. Pharm. Biopharm.* **75,** 173–178
6. Kigasawa, K., Kajimoto, K., Hama, S., Saito, A., Kanamura, K., and Kogure,

K. (2010) Noninvasive delivery of siRNA into the epidermis by iontophoresis using an atopic dermatitis-like model rat. *Int. J. Pharm.* **383,** 157–160
7. Hashim, I. I., Motoyama, K., Abd-Elgawad, A. E., El-Shabouri, M. H., Borg, T. M., and Arima, H. (2010) Potential use of iontophoresis for transdermal delivery of NF-kappaB decoy oligonucleotides. *Int. J. Pharm.* **393,** 127–134
8. Kajimoto, K., Yamamoto, M., Watanabe, M., Kigasawa, K., Kanamura, K., Harashima, H., and Kogure, K. (2011) Noninvasive and persistent transfollicular drug delivery system using a combination of liposomes and iontophoresis. *Int. J. Pharm.* **403,** 57–65
9. Kigasawa, K., Kajimoto, K., Nakamura, T., Hama S, Kanamura K, Harashima H, Kogure K. (2011) Noninvasive and efficient transdermal delivery of CpG-oligodeoxynucleotide for cancer immunotherapy. *J. Control. Release* **150,** 256–265
10. Kigasawa, K., Miyashita, M., Kajimoto, K., Kanamura, K., Harashima, H., and Kogure, K. (2012) Efficient intradermal delivery of superoxide dismutase using a combination of liposomes and iontophoresis for protection against UV-induced skin damage. *Biol. Pharm. Bull.* **35,** 781–785
11. Yamamoto, T., Saeki, Y., Kurasawa, M., Kuroda, S., Arase, S., and Sasaki, H. (2008) Effect of RNA interference of tight junction-related molecules on intercellular barrier function in cultured human keratinocytes. *Arch. Dermatol. Res.* **300,** 517–524
12. Tunggal, J. A., Helfrich, I., Schmitz, A., Schwarz, H., Günzel, D., Fromm, M., Kemler, R., Krieg, T., and Niessen, C. M. (2005) E-cadherin is essential for in vivo epidermal barrier function by regulating tight junctions. *EMBO J.* **24,** 1146–1156
13. Retamal, M. A., Schalper, K. A., Shoji, K. F., Bennett, M. V., and Sáez, J. C. (2007) Opening of connexin 43 hemichannels is increased by lowering intracellular redox potential. *Proc. Natl. Acad. Sci. U.S.A.* **104,** 8322–8327
14. Ohtake, K., Maeno, T., Ueda, H., Ogihara, M., Natsume, H., and Morimoto, Y. (2003) Poly-L-arginine enhances paracellular permeability via serine/threonine phosphorylation of ZO-1 and tyrosine dephosphorylation of occludin in rabbit nasal epithelium. *Pharm. Res.* **20,** 1838–1845
15. Tamura, A., Oishi, M., and Nagasaki, Y. (2009) Enhanced cytoplasmic delivery of siRNA using a stabilized polyion complex based on PEGylated nanogels with a cross-linked polyamine structure. *Biomacromolecules* **10,** 1818–1827
16. Solan, J. L., and Lampe, P. D. (2009) Connexin43 Phosphorylation: structural changes and biological effects. *Biochem. J.* **419,** 261–272
17. Laird, D. W. (2005) Connexin phosphorylation as a regulatory event linked to gap junction internalization and degradation. *Biochim. Biophys. Acta* **1711,** 172–182
18. Lampe, P. D., TenBroek, E. M., Burt, J. M., Kurata, W. E., Johnson, R. G., and Lau, A. F. (2000) Phosphorylation of connexin43 on serine368 by protein kinase C regulates gap junctional communication. *J. Cell Biology* **149,** 1503–1512
19. Solan, J. L., Lampe, P. D. (2005) Connexin phosphorylation as a regulatory event linked to gap junction channel assembly. *Biochim. Biophys. Acta* **1711,** 154–163
20. Inoue, N., Todo, H., Iidaka, D., Tokudome, Y., Hashimoto, F., Kishino, T., and Sugibayashi, K. (2010) Possibility and effectiveness of drug delivery to skin by needle-free injector. *Int. J. Pharm.* **391,** 65–72
21. De Vuyst, E., Wang, N., Decrock, E., De Bock, M., Vinken, M., Van Moorhem, M., Lai, C., Culot, M., Rogiers, V., Cecchelli, R., Naus, C. C., Evans, W. H., and Leybaert, L. (2009) Ca^{2+} regulation of connexin 43 hemichannels in C6 glioma and glial cells. *Cell Calcium* **46,** 176–187
22. El Maghraby, G. M., Barry, B. W., and Williams, A. C. (2008) Liposomes and skin: from drug delivery to model membranes. *Eur. J. Pharm. Sci.* **34,** 203–222
23. Sonaje, K., Chuang, E. Y., Lin, K. J., Yen, T. C., Su, F. Y., Tseng, M. T., and Sung, H. W. (2012) Opening of epithelial tight junctions and enhancement of paracellular permeation by chitosan: microscopic, ultra-structural and computed-tomographic observations. *Mol. Pharm.* **9,** 1271–1279
24. Peixoto, E. B., and Collares-Buzato, C. B. (2005) Protamine-induced epithelial barrier disruption involves rearrangement of cytoskeleton and decreased tight junction-associated protein expression in cultured MDCK strains. *Cell Struct. Funct.* **29,** 165–178
25. Nagasawa, K., Chiba, H., Fujita, H., Kojima, T., Saito, T., Endo, T., and Sawada, N. (2006) Possible involvement of gap junctions in the barrier function of tight junctions of brain and lung endothelial cells. *J. Cell Physiol.* **208,** 123–132
26. Park, J. H., Lee, M. Y., Heo, J. S., and Han, H. J. (2008) A potential role of connexin 43 in epidermal growth factor-induced proliferation of mouse embryonic stem cells: Involvement of Ca^{2+}/PKC, p44/42 and p38 MAPKs pathways. *Cell Prolif.* **41,** 786–802
27. Kirn-Safran, C., Farach-Carson, M. C., and Carson, D. D. (2009) Multifunctionality of extracellular and cell surface heparan sulfate proteoglycans. *Cell Mol. Life Sci.* **66,** 3421–3434
28. Lurtz, M. M., and Louis, C. F. (2003) Calmodulin and protein kinase C regulate gap junctional coupling in lens epithelial cells. *Am. J. Physiol. Cell Physiol.* **285,** C1475–C1482
29. Li, C., Fultz, M. E., Parkash, J., Rhoten, W. B., and Wright, G. L. (2001) Ca^{2+}-dependent actin remodeling in the contracting A7r5 cell. *J. Muscle Res. Cell Motil.* **22,** 521–534
30. Hartsock, A., and Nelson, W. J. (2008) Adherens and tight junctions: structure, function and connections to the actin cytoskeleton. *Biochim. Biophys. Acta* **1778,** 660–669
31. Miyoshi, J., and Takai, Y. (2008) Structural and functional associations of apical junctions with cytoskeleton. *Biochim. Biophys. Acta* **1778,** 670–691